Journal of Biomechanics 99 (2020) 109502

Contents lists available at ScienceDirect

Journal of Biomechanics

journal homepage: www.elsevier.com/locate/jbiomech
www.JBiomech.com

A modular impact diverting mechanism for football helmets

Daniel E. Abram *, Adrian Wikarna, Farid Golnaraghi, G. Gary Wang

Head Injury Prevention Laboratory, Simon Fraser University, Surrey, BC V3T 0A3, Canada

ARTICLE INFO

Article history:
Accepted 7 November 2019

Keywords:
Helmet
Oblique impact
Rotational acceleration
Concussion
Traumatic brain injury

ABSTRACT

To mitigate the injurious effect of the rotational acceleration of the brain, a modular Impact Diverting Mechanism (IDM) has been developed. The IDM can replace stickers (decals) that normally attach to the exterior of a football helmet. The IDM decals reduce friction and catch points between the covered area with the IDM on the outer shell of the helmet and the impacting surface, thereby decreasing rotational acceleration acting on the player's head. A Riddell Speed helmet's exterior was prepared with the IDM and outfitted to a headform equipped with linear accelerometers and gyroscopes. The helmets were tested at an impact velocity of 5.5 m/s at 15°, 30°, and 45° to the vertical: on the front, side, and back of the helmet. Results of 135 impact tests in the lab show that the IDM decal, when compared to helmets without it, reduced the rotational acceleration, rotational velocity, SI, HIC, and RIC ranging from 22% to 77%, 20% to 74%, 13% to 68%, 7% to 68%, 31% to 94%, respectively. Protection against rotational acceleration from oblique impacts is not prioritized in modern football helmets, as evident by current standard helmet testing protocols. This study demonstrates that the inclusion of the IDM decals in football helmets can help reduce the effects of rotational acceleration of the head during oblique impacts.

1. Introduction

American football players are often at risk of the short and long-term effects of head injury and concussion. Football helmet designs over the past 30 years have been mainly focusing on the wearers' protection against injuries resulting from excessive translational acceleration, such as intracranial hemorrhaging and skull fracture. However, rotational accelerations of the brain are also known to be among the key factors behind head injury and concussion (Holbourn et al., 1943; COST 327, 2001; Kleiven, 2007; Kleiven, 2013). Rotational acceleration of the head introduces shear stress on cranial tissues resulting in Subdural Hematoma (SDH) and Diffuse Axonal Injury (DAI). As the brain's bulk modulus (resistance to uniform compression) is nearly one million times higher than that of the shear modulus (McElhaney et al., 1976), brain tissue is much more susceptible to injury from shear forces than to compression caused by purely linear motion (Gennarelli et al., 1987; Kleiven, 2007). Early testing on primates demonstrated the clear role of rotational acceleration in the generation of concussion, SDH, and DAI (Ommaya and Hirsch, 1971; Ommaya et al., 1973; Margulies and Thibault, 1992). McKee et al. (2009) reviewed cases surrounding head injuries sustained by athletes and found a strong link between Chronic Traumatic Encephalopathy (CTE) in football players and combat veterans with a repeated concussion. Sufferers of CTE incur life-long neurodegenerative effects, including memory loss, impaired judgment, impulse control problems, aggression, depression, suicidality, parkinsonism, and, eventually, progressive dementia (Stern et al., 2011). The rising incidence of concussions, which accounts for over 1.6 – 1.8 million sports-related head injuries each year within the United States (Langlois et al., 2006), substantiates a need to address the lack of industry solutions to rotational damping mechanisms in modern helmets.

Nearly all impacts to the helmet are at an angle, inducing both linear and rotational acceleration and magnifying the strain on a player's brain. When helmets strike an obstacle obliquely, the exerted force comprises two components: normal and tangential (Otte, 1991). If the exerted force passes through the center of gravity (CG) of the object (helmeted head), the object will only experience linear acceleration (Scenario 1). Such impacts rarely occur, and the exerted force does not generate torque or rotational acceleration. However, if the force would not pass through the CG (off-centred force), then the force results in both rotational and linear acceleration of the head (Scenario 2). In addition to the rotational acceleration caused by the off-centred force during Scenario 2 impacts, the surface condition of the object can result in further rotation of the object. As shown in a 2008 study by Finan et al. (2008) for a majority of the cases, an increase in the friction coefficient of an object's (helmet) surface can increase the total

* Corresponding author at: School of Mechatronics Systems Engineering, Simon Fraser University, 102 Ave, Surrey, BC V3T 0A3, Canada.

E-mail address: dabramm@gmail.com (D.E. Abram).

https://doi.org/10.1016/j.jbiomech.2019.109502
0021-9290/

experienced rotational acceleration. The magnitude of the generated rotational acceleration depends on the location and orientation of an impact force, as well as the surface condition of the colliding objects (Hibbeler, 2016). Therefore, it is recommended to reduce the friction between the surface of a helmet and the contacting obstacle.

Both the magnitude and duration of an impact play important roles in causing a head injury. The human brain can withstand relatively high linear and rotational acceleration for time intervals less than five milliseconds (Gurdjian et al., 1966; O'Riodain et al., 2003; Hitosugi et al., 2014). However, in football, typical impacts last for around 10–15 ms, further increasing the possibility of sustaining brain injuries (Pellman et al., 2003b, 2003a; Zhang et al., 2004). Other studies suggest that rotational velocity has a substantial correlation to brain strain response and is therefore critical for anticipating brain injury as a result of impact events (Kleiven, 2007; Ji et al., 2014; Rowson et al., 2012; Hardy et al., 2007). Rotational velocity can help distinguish short interval impacts from the long and more injurious impacts that have the same magnitudes of rotational acceleration.

Current football helmets offer inadequate protection against impacts that produce head rotations and only partially solve the issue of head injury. The impact testing methodologies imposed on manufactured football helmets consider vertical drops onto a flat surface; hence, the effects of high-magnitude translational acceleration are emphasized in design and testing for the market (NOCSAE, 2017). On the other hand, standards for evaluating helmets in angled (oblique) drop impact scenarios have not yet been established and widely accepted. The National Operating Committee on Standards for Athletic Equipment (NOCSAE) has made efforts to amend their standard testing procedures to include rotational acceleration measurement, and it is supposed to come into effect in November 2019.

Current research, such as by Johnston et al., has integrated damping methods directly into modified football helmets. These modified helmets function through a 3D fibre network foam technology within the lining of the helmet, which is intended to disconnect the head and the helmet under substantial oblique impact forces (Johnston et al., 2015). The modified helmet achieves a 33.6% average attenuation of rotational acceleration at about 3.2 m/s; however, higher impact speeds remain untested. A study by Siegkas et al. tested the efficacy of a novel helmet liner accessory consisting of two dilatant viscoelastic disks, which can potentially enhance the protection offered by regular helmets (Siegkas et al., 2019). Outcomes of the testing have shown significant reductions of peak accelerations for both low-speed and high-speed frontal impacts—4.35 m/s and 7.5 m/s, respectively—and for high-speed side impacts with the inclusion of the viscoelastic components. However, the tested samples were limited due to the helmet costs, and performing additional tests were suggested by the authors. Industry solutions, such as the Multi-Directional Impact Protection System (MIPS) platform, offer a slip plane between the user and helmet to provide a similar damping effect (Halldin, 2011; Phillips, 1997). The technology has been widely commercialized for cycling, motorcycling, and skiing helmets, however, it is not clear if it could be applied to the football helmets.

An approach was taken to mitigate the injurious effect of rotational acceleration by replacing conventional decal with a decal made of a micro-engineered film. The proposed patented design is called impact diverting mechanism (IDM) (Golnaraghi et al., 2012) and is composed of several layers of polymer films and a medium in between, as shown in Fig. 1. These components provide a low-friction interface between the interacting layers upon receiving an oblique impact, thereby behaving like an intermediary layer that reduces the amount of friction force transferred from the impacting surface to the outer shell of the helmet. The system can replace conventional sports decals or stickers used by football teams on their helmets. This study examines the performance of the IDM applied to a football helmet and outlines the results of the oblique impact tests.

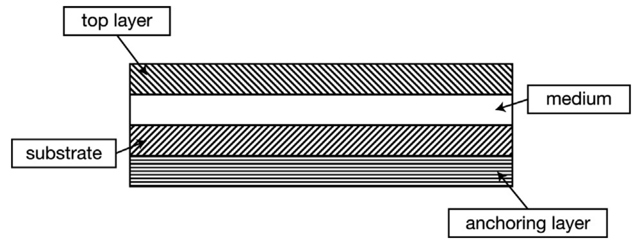

Fig. 1. Cross-section of the structure of the membrane, detailing the layout of the top, medium, substrate, and anchoring layers.

2. Materials and methods

2.1. IDM material development

The IDM is designed to attenuate rotational acceleration by decoupling the outer shell from the impacting surface during oblique impacts. The technology consists of four layers; top (outer) layer, medium, substrate, and anchoring layer, as shown in Fig. 1. The top layer consists of a material that experimentally found to provide the surface condition, elongation, and tensile strength required to mitigate rotational acceleration during high-speed impact loading. These characteristics allow stretching and sliding of the top layer during impact on an oblique impact surface. The medium between the top layer and substrate reduces the friction between segments. This facilitates the sliding of the top layer with respect to the substrate. The anchoring lower layer uses a peel-and-stick adhesive to attach the system to the exterior of a helmet. Fig. 2-a shows the IDM attached to the outer shell of the helmet using peel-and-stick adhesive, followed by Fig. 2-b, which shows a force applied on the IDM. As soon as the force is removed from the IDM, it goes back to its original form. Fig. 2 shows an IDM sample in a teardrop shape; however, it can have any shape or graphics.

2.2. Equipment

A test rig for performing oblique impact tests was developed (patent-pending) and constructed at the Head Injury Prevention (HIP) Lab at the School of Mechatronics Systems Engineering,

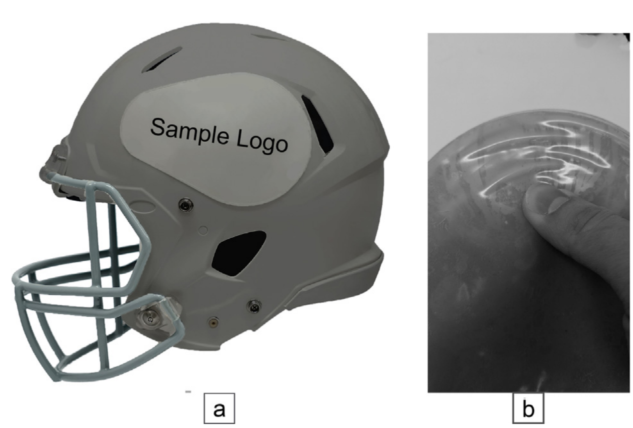

Fig. 2. IDM sample (a) attached to a helmet, (b) displaying the sliding characteristics of the IDM under a load.

Simon Fraser University (SFU), and is named Suspend-X. Fig. 3 details the test rig. Unlike other drop testing equipment, Suspend-X does not have a basket frame—connected to the drop carriage assembly—to support an oriented helmeted headform. Instead, the helmeted headform is suspended from an extended arm and released right before impact. This allows Suspend-X to perform impact tests at sharp angles, which may not be suitable for most conventional basket-style test rigs. For instance, performing an impact test at 15° to the vertical with a basket support frame can result in the helmeted headform hitting the frame after bouncing from the anvil, causing damage to the equipment.

Oblique impacts were conducted using a 42 Shore A Modular Elastomer Programmer (MEP) pad installed on an anvil angled 15°, 30°, and 45° to the vertical. The MEP pad is the NOCSAE standard impact surface. Falls were conducted at speeds of 5.5 m/s according to test procedures defined for football helmets (NOCSAE, 2017). The impact velocities of each drop were measured using a photoelectric time gate adjacent to the rail guide. A high-speed camera (Edgertronics SC2+), capable of recording at 4000 frames/sec in high definition, was used to monitor the quality of each impact.

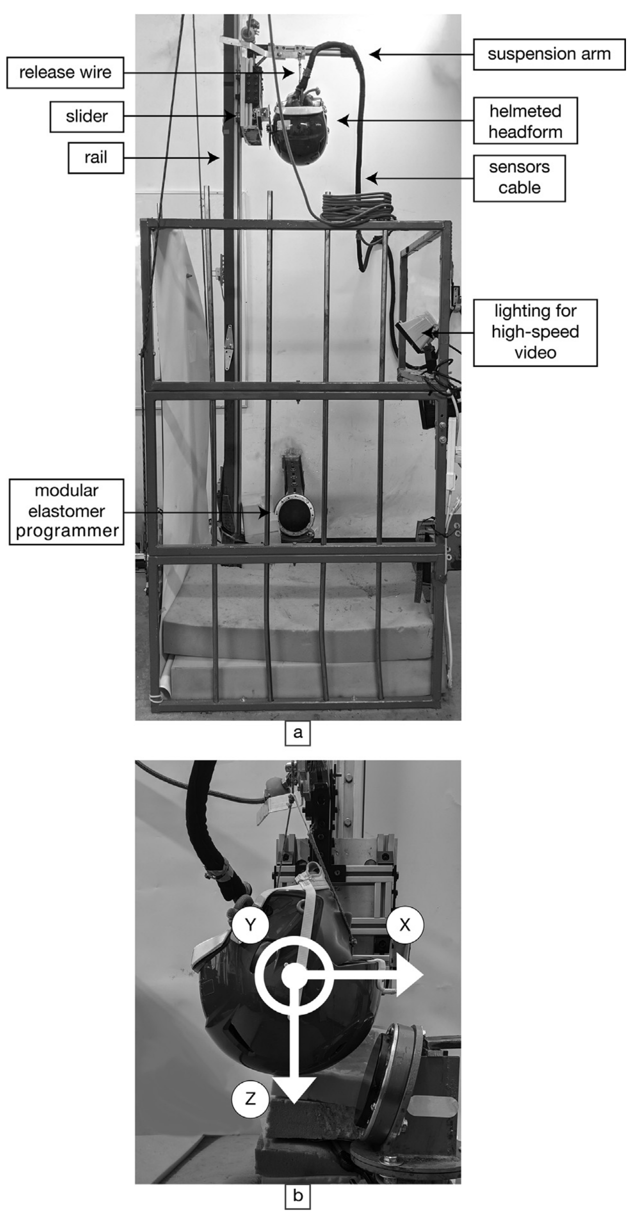

Fig. 3. (a) Suspend-X oblique impact test rig, (b) A helmeted Hybrid III headform suspended just above the impact surface with the reference measurement axis.

The headform was a 50th percentile adult male Hybrid III with a removable vinyl skin which has an average thickness of 10 mm purchased from Humanetics Innovative Solutions. The importance of surface condition has also been studied by Ebrahimi et al. (2015), showing that surface condition plays a significant role in the impact conditions of the headform. Research has shown that a headform (similar to the one used) without a neck can be used as a suitable replacement for a full-body dummy (Aare and Halldin, 2003; COST 327, 2001).

The surrogate headform was equipped with nine single-axis linear accelerometers (ENDEVCO 7204C), arranged in a 3–2–2–2 array to measure the headform's linear ($a(t)$) and calculate rotational acceleration ($\alpha(t)$) in x, y, and z-axes according to the algorithm proposed by Padgaonkar et al. (1975). In addition, the tested Hybrid III headform was equipped with three single-axis gyroscopes to measure the headform's rotational velocity ($\omega(t)$) in x, y, and z axes. Headform measurements were collected at a sampling rate of 20 kHz with a National Instrument data acquisition (DAQ) system, and a custom program based on LabView software controlled the data capturing and post-processing. The gyroscope data was filtered through a 289 Hz low-pass filter as recommended by Cobb et al. (2018), and noise from the linear accelerometer input signals was reduced using a standard 1000 Hz low-pass filter following SAE J211 (NOCSAE, 2017).

2.3. Methodology

A Riddell Speed football helmet, Size L, was used in testing. Depending on the test configuration, a conventional decal (0.4 mm thick) or an IDM (0.63 mm thick) would be attached to the outer shell of the helmet using peel-and-stick adhesive. Then, the helmeted headform was placed onto the suspension arm of the drop test rig. Orientation and positioning were secured and levelled by laser and other levelling equipment. The suspension arm was then lifted to a height to produce an impact speed of 5.5 m/s with the anvil.

Some researchers divided the football helmet into distinct regions and examined the distribution of impacts relative to the specified areas (Crisco et al., 2010; Daniel et al., 2012; Pellman et al., 2003b, 2003a, part 2). According to these studies, the critical areas include the lateral, front, rear, and top portions of the helmets. In this work, three regions were selected for testing based on the three most prevalent impact locations: the Front-Y (FY), Lateral-X (LX), and Side-Back (SB). For each selected region, the helmet was tested at three separate impact angles: 15°, 30°, and 45° to the vertical (as shown in Fig. 4). For each impact scenario, three different helmet configurations were tested: helmet without any modification (BARE), helmet with conventional decal made of vinyl (CONV) and helmet with Impact Diverting Mechanism (IDM). With five trials for each category, 135 tests were conducted in total.

To approximate the probability of head and brain injury, the Gadd Severity Index (SI) (Gadd, 1966) the Head Injury Criterion (HIC) (McHenry, 2004), Rotational Injury Criterion (RIC) (Kimpara and Iwamoto, 2012), Brain Injury Criterion (BrIC), and the probability of sustaining an Abbreviated Injury Score (AIS) 2 brain injury (P (AIS 2)) (Takhounts et al., 2013) were determined. The SI, HIC, RIC, BrIC, and P(AIS 2) were calculated with Eqs. (1), (2), (3), and (4), respectively.

$$SI = \int_0^T a(t)^{2.5} dt \tag{1}$$

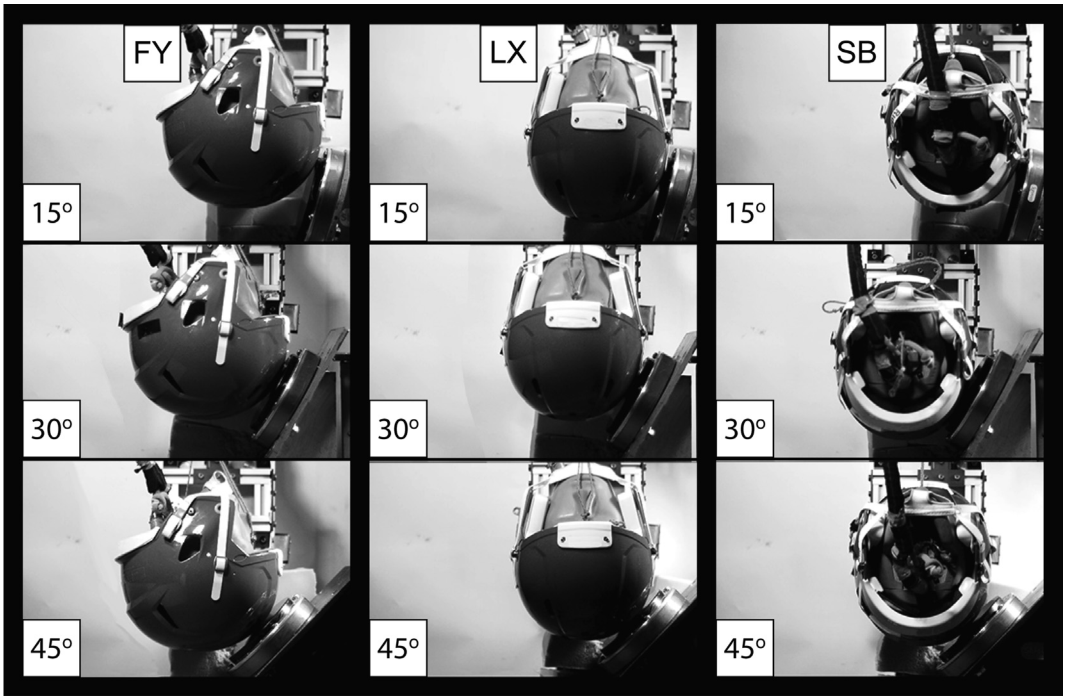

Fig. 4. Nine impact scenarios. Locations of impacts on the helmet.

$$HIC = \left[(t_2 - t_1) \left\{ \frac{1}{(t_2 - t_1)} \int_{t_1}^{t_2} a(t) dt \right\}^{2.5} \right]_{max} \tag{2}$$

$$RIC = \left[(t_2 - t_1) \left\{ \frac{1}{(t_2 - t_1)} \int_{t_1}^{t_2} \alpha(t) dt \right\}^{2.5} \right]_{max} \tag{3}$$

$$BrIC = \sqrt{\left(\frac{\omega_x}{66.25}\right)^2 + \left(\frac{\omega_y}{56.45}\right)^2 + \left(\frac{\omega_z}{42.87}\right)^2} \tag{4}$$

$$P(AIS2) = 1 - e^{-\left(\frac{BrIC}{0.567}\right)^{2.84}} \tag{5}$$

where

t = time ω_x = rotational velocity in x
$a(t)$ = linear acceleration ω_y = rotational velocity in y
$\alpha(t)$ = rotational acceleration ω_z = rotational velocity in z

The integral time is the duration that the main event of impact takes place, and it can vary by the type of helmet and speed of impact. Some research studies suggested 15 ms and 36 ms for the integral time limit of HIC and RIC, respectively (Kimpara and Iwamoto, 2012; Prasad and Mertz, 1985). All 135 impact tests on the Riddell Speed football helmet were studied, and results showed

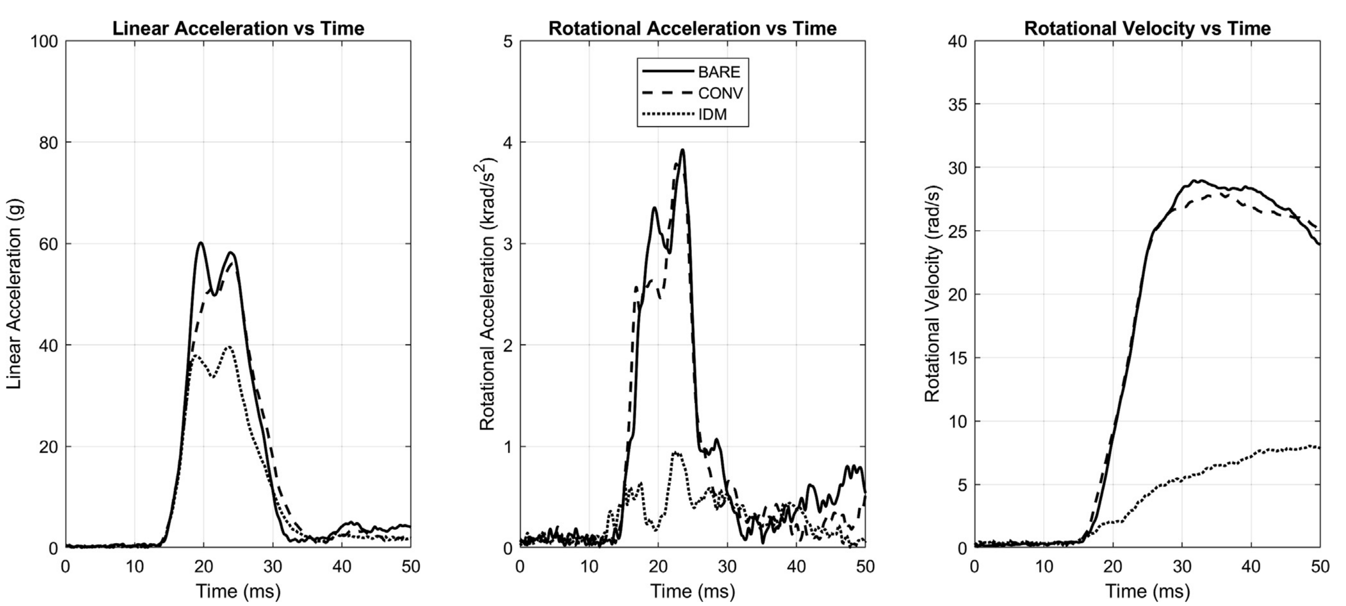

Fig. 5. Sample linear acceleration, rotational acceleration, and rotational velocity curves for BARE, CONV, and IDM.

Table 1
Summary of all results from Front-Y impact tests.

		15°				30°				45°			
		Avg	STDEV	Red (%)	p-value	Avg	STDEV	Red (%)	p-value	Avg	STDEV	Red (%)	p-value
Resultant ROT. ACC. (krad/s^2)	BARE	3.33	0.14	–	–	3.94	0.32	–	–	4.25	0.19	–	–
	CONV	3.50	0.29	−5.0	0.2878	3.56	0.08	9.7	0.0320	4.36	0.19	−2.7	0.3720
	IDM	1.71	0.03	48.8	<0.001	2.87	0.27	27.2	<0.001	3.02	0.15	28.9	<0.001
Resultant ROT. VEL. (rad/s)	BARE	34.72	0.93	–	–	33.03	0.99	–	–	27.32	0.37	–	–
	CONV	34.98	1.19	−0.8	0.7076	32.89	0.59	0.4	0.7959	27.69	0.21	−1.4	0.0806
	IDM	10.31	1.04	70.3	<0.001	12.40	1.17	62.5	<0.001	16.00	0.98	41.4	<0.001
Resultant LIN. ACC. (g)	BARE	34.91	1.45	–	–	62.99	3.97	–	–	86.66	0.89	–	–
	CONV	36.35	3.12	−4.1	0.3776	58.71	1.37	6.8	0.0518	85.24	3.18	1.6	0.3657
	IDM	31.85	1.66	8.3	0.0146	56.61	1.70	10.1	0.0107	80.48	5.73	7.1	0.0445
SI	BARE	52.10	2.76	–	–	152.29	22.46	–	–	304.50	13.17	–	–
	CONV	52.57	4.74	−0.9	0.8510	128.08	4.63	15.9	0.0459	294.34	18.44	3.3	0.3457
	IDM	31.48	3.11	39.6	<0.001	132.27	8.53	13.1	0.0995	261.83	27.26	14.0	0.0136
HIC_{20}	BARE	26.86	1.26	–	–	63.77	5.23	–	–	114.16	2.71	–	–
	CONV	26.75	2.00	0.5	0.8979	58.58	1.16	8.1	0.0620	108.88	2.18	4.6	0.0094
	IDM	15.18	0.81	43.6	<0.001	54.66	2.92	14.3	0.0093	105.71	4.50	7.4	0.0070
RIC_{20}	BARE	2.53e6	1.37e5	–	–	2.56e6	2.47e5	–	–	1.76e6	5.52e4	–	–
	CONV	2.69e6	2.20e5	−6.4	0.1938	2.48e6	8.61e4	3.2	0.5029	1.84e6	1.08e5	−4.5	0.1882
	IDM	2.29e5	4.39e4	90.9	<0.001	4.91e5	2.85e4	80.8	<0.001	6.84e5	1.53e5	61.1	<0.001
BrIC	BARE	0.6164	0.0167	–	–	0.5848	0.0178	–	–	0.4850	0.0067	–	–
	CONV	0.6214	0.0208	−0.8	0.6910	0.5830	0.0105	0.3	0.8470	0.4930	0.0025	−1.6	0.0372
	IDM	0.1854	0.0188	69.9	<0.001	0.2184	0.0209	62.6	<0.001	0.2835	0.0173	41.5	<0.001
P (AIS2)	BARE	0.7180	0.0274	–	–	0.6640	0.0316	–	–	0.4736	0.0132	–	–
	CONV	0.7258	0.0340	−1.1	0.7012	0.6610	0.0188	0.4	0.8614	0.4894	0.0050	−3.3	0.0370
	IDM	0.0417	0.0116	94.2	<0.001	0.0655	0.0163	90.1	<0.001	0.1311	0.0207	72.3	<0.001

Table 2
Summary of all results from Lateral-X impact tests.

		15°				30°				45°			
		Avg	STDEV	Red (%)	p-value	Avg	STDEV	Red (%)	p-value	Avg	STDEV	Red (%)	p-value
Resultant ROT. ACC. (krad/s^2)	BARE	3.55	0.17	–	–	3.53	0.08	–	–	3.29	0.15	–	–
	CONV	3.57	0.13	−0.4	0.8861	3.48	0.19	1.5	0.5863	3.37	0.16	−2.4	0.4373
	IDM	0.84	0.05	76.3	<0.001	0.80	0.18	77.3	<0.001	1.52	0.40	53.9	<0.001
Resultant ROT. VEL. (rad/s)	BARE	34.39	0.51	–	–	28.60	0.85	–	–	22.69	0.70	–	–
	CONV	34.00	0.27	1.1	0.1769	27.94	0.21	2.3	0.1266	23.08	0.25	−1.7	0.2712
	IDM	14.15	0.63	58.8	<0.001	9.60	1.46	66.4	<0.001	5.99	2.36	73.6	<0.001
Resultant LIN. ACC. (g)	BARE	39.28	0.98	–	–	59.51	2.36	–	–	72.52	3.41	–	–
	CONV	39.51	1.07	−0.6	0.7254	56.74	1.85	4.7	0.0724	70.17	1.68	3.2	0.2048
	IDM	24.11	2.20	38.6	<0.001	39.93	2.30	32.9	<0.001	65.44	2.49	9.8	0.0056
SI	BARE	69.84	1.63	–	–	194.34	9.97	–	–	289.17	23.62	–	–
	CONV	68.71	4.85	1.6	0.6236	171.10	13.33	12.0	0.0142	283.66	11.71	1.9	0.6527
	IDM	22.62	2.21	67.6	<0.001	77.02	6.80	60.4	<0.001	213.73	5.79	26.1	<0.001
HIC_{20}	BARE	47.77	2.08	–	–	103.54	1.77	–	–	142.61	9.61	–	–
	CONV	46.45	1.50	2.8	0.2833	99.77	5.15	3.6	0.1594	141.81	4.17	0.6	0.8686
	IDM	15.25	0.75	68.1	<0.001	47.55	2.11	54.1	<0.001	103.29	4.91	27.6	<0.001
RIC_{20}	BARE	3.37e6	1.22e5	–	–	2.18e6	1.62e5	–	–	1.50e6	1.05e5	–	–
	CONV	3.26e6	1.61e5	3.3	0.2414	2.10e6	5.97e4	3.6	0.3237	1.55e6	1.78e5	−3.2	0.6005
	IDM	1.92e5	2.24e4	94.3	<0.001	1.23e5	2.52e4	94.4	<0.001	2.31e5	1.09e5	72.7	<0.001
BrIC	BARE	0.6085	0.0105	–	–	0.5012	0.0143	–	–	0.4047	0.0167	–	–
	CONV	0.6085	0.0040	0.0	0.9938	0.4968	0.0058	0.9	0.5416	0.4112	0.0041	−1.6	0.4200
	IDM	0.2789	0.0138	54.2	<0.001	0.1991	0.0276	60.3	<0.001	0.1105	0.0459	72.7	<0.001
P (AIS2)	BARE	0.7053	0.0179	–	–	0.5056	0.0283	–	–	0.3191	0.0300	–	–
	CONV	0.7054	0.0067	0.0	0.9892	0.4969	0.0115	1.7	0.5416	0.3308	0.0076	−3.7	0.4239
	IDM	0.1253	0.0163	82.2	<0.001	0.0517	0.0199	89.8	<0.001	0.0133	0.0171	95.8	<0.001

that the duration of the impact is less than 20 ms for the impact speed of 5.5 m/s. Fig. 5 shows a sample linear acceleration, rotational acceleration, and rotational velocity curves for BARE, CONV, and IDM.

3. Results and discussion

Tables 1 to 3 summarize the results of all the testing categories and compare the results obtained for Riddell Speed helmets with

Table 3
Summary of all results from Side-Back impact tests.

		15°				30°				45°			
		Avg	STDEV	Red (%)	p-value	Avg	STDEV	Red (%)	p-value	Avg	STDEV	Red (%)	p-value
Resultant ROT. ACC. (krad/s^2)	BARE	3.30	0.12	–	–	3.04	0.21	–	–	3.53	0.07	–	–
	CONV	3.27	0.15	0.9	0.7183	2.93	0.26	3.7	0.4623	3.27	0.34	7.6	0.1790
	IDM	1.51	0.12	54.3	<0.001	1.78	0.28	41.4	<0.001	2.41	0.26	31.9	<0.001
Resultant ROT. VEL. (rad/s)	BARE	33.24	0.61	–	–	29.98	1.99	–	–	22.79	0.85	–	–
	CONV	33.14	0.46	0.3	0.7948	29.54	0.59	1.4	0.6538	21.74	0.93	4.6	0.0985
	IDM	19.13	1.76	42.4	<0.001	17.26	3.28	42.4	<0.001	18.28	1.90	19.8	0.0013
Resultant LIN. ACC. (g)	BARE	29.73	0.33	–	–	48.27	1.08	–	–	67.87	1.48	–	–
	CONV	29.52	0.66	0.7	0.5304	48.26	1.90	0.0	0.9953	69.03	0.80	−1.7	0.1642
	IDM	20.02	1.13	32.7	<0.001	43.17	1.18	10.6	<0.001	56.43	0.68	16.9	<0.001
SI	BARE	48.60	2.80	–	–	135.77	12.51	–	–	275.09	3.12	–	–
	CONV	49.00	3.59	−0.8	0.8499	142.04	10.86	−4.6	0.4217	286.72	10.17	−4.2	0.0404
	IDM	16.13	1.51	66.8	<0.001	78.64	3.32	42.1	<0.001	159.77	4.97	41.9	<0.001
HIC_{20}	BARE	77.30	4.74	–	–	243.51	23.95	–	–	504.25	4.46	–	–
	CONV	78.38	6.57	−1.4	0.8150	255.70	21.56	−5.0	0.2883	524.44	19.44	−4.0	0.0724
	IDM	26.11	2.75	66.2	<0.001	138.17	5.89	43.3	<0.001	287.78	9.32	42.9	<0.001
RIC_{20}	BARE	0.1682	0.0163	–	–	0.1582	0.0420	–	–	0.1131	0.0115	–	–
	CONV	0.1663	0.0237	1.1	0.4061	0.1577	0.0131	0.3	0.9222	0.1119	0.0107	1.1	0.7791
	IDM	0.0309	0.0079	81.7	0.0192	0.0626	0.0283	60.4	0.0036	0.0786	0.0237	30.5	0.0237
BrIC	BARE	0.7720	0.0133	–	–	0.6935	0.0497	–	–	0.5252	0.0195	–	–
	CONV	0.7707	0.0077	0.2	0.8551	0.6871	0.0144	0.9	0.7897	0.5026	0.0217	4.3	0.1216
	IDM	0.4205	0.0258	45.5	<0.001	0.3350	0.0547	51.7	<0.001	0.3128	0.0257	40.4	<0.001
P (AIS2)	BARE	0.9092	0.0104	–	–	0.8245	0.0665	–	–	0.5525	0.0381	–	–
	CONV	0.9084	0.0063	0.1	0.8895	0.8215	0.0183	0.4	0.9254	0.5082	0.0426	8.0	0.1218
	IDM	0.3488	0.0486	61.6	<0.001	0.2073	0.0850	74.9	<0.001	0.1702	0.0352	69.2	<0.001

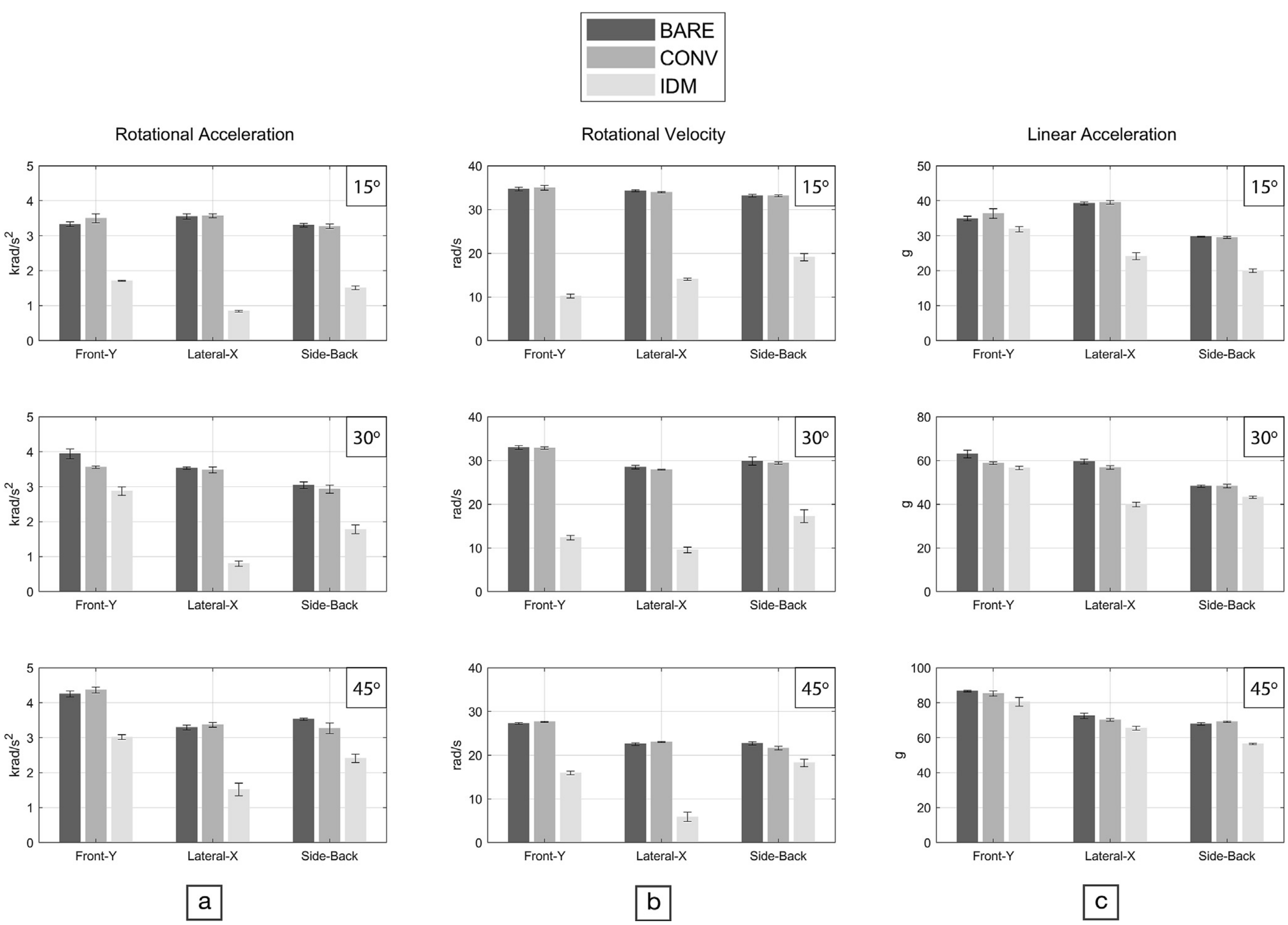

Fig. 6. Testing results: (a) resultant rotational acceleration, (b) resultant rotational velocity, and (c) resultant linear acceleration.

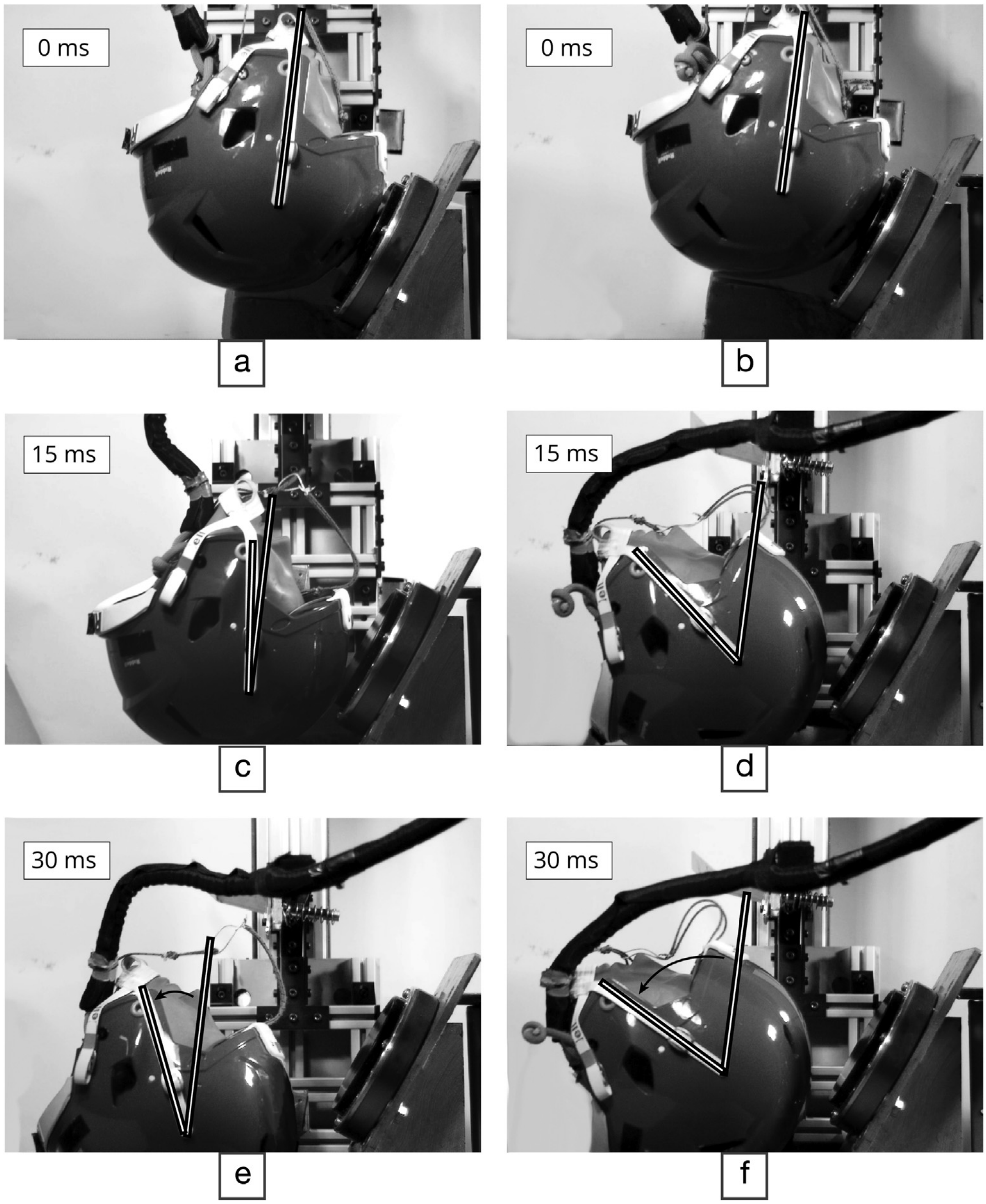

Fig. 7. Side by side comparison of a helmet with IDM (left side) and without (right side): (a) and (b) moment of impact; (c) and (d) 15 ms after impact; (e) and (f) 30 ms after impact.

no surface change (BARE), with a conventional decal (CONV) and with the IDM decal. The performance of CONV and IDM was quantified by calculating the percent reduction (Red %) compared to BARE in all parameters measured (resultant rotational acceleration, resultant rotational velocity, resultant linear acceleration, HIC-20, RIC-20, SI, BrIC, and P(AIS 2)).

For all the measured parameters, conventional helmet decals did not produce a meaningful performance improvement. On the other hand, significant performance improvement was observed with the inclusion of the IDM in all impact scenarios. The IDM decal resulted in a reduction of rotational acceleration ranging from 27% to 77%, decreasing from 3.53 krad/s^2 for BARE to 0.80 krad/s^2 which is considerably lower than the head injury (concussion) threshold of 4.5 to 6.0 krad/s^2 as defined in different research studies (Pellman et al., 2003b, 2003a; Rowson and Duma, 2013; Zhang et al., 2004).

The IDM with a thickness of 0.63 mm has a negligible compression under the normal force. However, in all impact scenarios, there was a 7% to 39% reduction in linear acceleration. The reason for such reductions in linear acceleration is believed to be the fact that the IDM, compared to CONV and BARE, allows the impacting object to slide on a larger area on a helmet outer shell. Therefore, the impacting force distributes over a larger area of the helmet shell and allows the impact-absorbing liner of the helmet to be more effective.

The IDM also produced a significant reduction in rotational velocity, SI, HIC, and RIC. On average, the IDM reduced the rotational velocity ranging from 20% to 74%, SI ranging from 13% to 68%, HIC ranging from 7% to 68%, and RIC ranging from 31% to 94%. Additionally, the HIC with a 15-ms integral time limit (HIC-15) was compared to the mainly examined 20-ms integral time limit (HIC-20), and similarly for the RIC with a 36-ms integral time limit (RIC-36) compared to the RIC-20. The comparison showed that there was less than 5% difference in performance for all measured parameters.

The IDM decal reduces the coefficient of friction between the interacting surfaces (impactor and helmet shell) and has no significant effect on the normal force component. The results showed that the reduction of the frictional force component yields a significant reduction in the rotational acceleration of the helmeted headform. For the type of impacts tests performed in this study, the frictional forces outweighed the role that off-centred normal forces play in causing rotational acceleration of the head. This shows that the surface condition of the outer shell of a helmet can contribute to the overall rotational acceleration exerted to a helmet. Fig. 6 shows the average peak value and variability (through error bars) of rotational acceleration, rotational

High-speed video footage of each test was used to verify the quality of the impact. The reduction of the measured parameters (especially rotational acceleration and rotational velocity) can be confirmed to some extent by examining the video footage. Fig. 7 shows some of the frames taken in the first 30 ms after two impacts, one with the IDM decal and the other one without the IDM decal.

For the purpose of this study, a Riddell Speed helmet was used for testing. According to the NOCSAE, the standard impact velocity in a football helmet certification test is 5.5 m/s (NOCSAE, 2017). Becker et al. (2015) has shown that if a helmet performs in severe impacts, then the same helmet is considered protective for all impacts of equal or lesser severity. Therefore, impact tests with lower than 5.5 m/s impact speed may not provide more insight into the performance of the helmet.

Currently, the size of the IDM has been limited to the size of the conventional football decals. Further implementation of the IDM could be made to cover the entire outer surface of the helmet. With this may come installation difficulty from end-users for replacing the damaged IDM. Research studies by Pellman et al. on NFL teams lay out key areas of a football helmet most commonly impacted. Using this information, the lateral left and right of a helmet, commonly covered by decorative decals, encompass these key areas (Crisco et al., 2010; Daniel et al., 2012; Pellman, 2016; Pellman et al., 2003b, 2003a). This furthers the practicality of the usage of the IDM as a decal in football.

The IDM is designed to be a disposable product, and a substantial impact can damage the top layer. When the IDM decal gets damage it is recommended to replace the damaged IDM as soon as possible.

4. Conclusion

Rotational acceleration of the head during oblique impacts has not been the center of attention in the football helmet design. Therefore, there is no mechanism in current football helmets to reduce the rotational acceleration of the head during impact. In this work, an impact diverting mechanism (IDM) in the form of a decal was introduced. The IDM decal looks similar to the conventional decals, can be installed on the other shell of a football helmet. Oblique impact tests were performed on helmets equipped with the IDM decals, conventional decals, and no decals. The results showed that conventional decals do not positively affect the performance of a helmet. However, the IDM decals can mitigate the rotational and linear acceleration of the head by up to 77% and 39%, respectively. The results also indicate that rotational acceleration caused by the frictional forces, compared to the off-centred normal forces, can be significant, and mitigating friction at the impact surface can enhance the protection of a football helmet.

Declaration of Competing Interest

Three of the authors (Daniel E. Abram, Farid Golnaraghi, and G. Gary Wang) are co-inventors of the IDM technology described in this manuscript and have filed patents and have a financial interest in the company that owns the technology.

Acknowledgments

This work was supported in part by grants from MITACS and the Natural Sciences and Engineering Council of Canada.

References

Aare, M., Halldin, P., 2003. A new laboratory rig for evaluating helmets subject to oblique impacts. Traffic Inj. Prev. 4 (3), 240–248.
COST 327, 2001. Motorcycle Safety Helmet, Luxembourg: Office for Official Publications of the European Communities.
Becker, E.B., Anishchenko, D.V., Palmer, S.B., 2015. Motorcycle Helmet Impact Response at Various Levels of Severity for Different Standard Certifications. INTERNATIONAL RESEARCH COUNCIL ON BIOMECHANICS OF INJURY. In press.
Cobb, B., Tyson, A., Rowson, S., 2018. Head acceleration measurement techniques: reliability of angular rate sensor data in helmeted impact testing. J. Sports Eng. Technol. 232 (2), 176–181.
Crisco, J.J., Fiore, R.R., Beckwith, J.G., Chu, J.J., Brolinson, P.G., Duma, S., McAllister, T. W., Duhaime, A.C., Greenwald, R.M., 2010. Frequency and location of head impact exposures in individual collegiate football players. J. Athletic Train. 45 (6), 549–559.
Daniel, R.W., Rowson, S., Duma, S.M., 2012. Head impact exposure in youth football. Ann. Biomed. Eng. 40 (4), 976–981.
Ebrahimi, I., Golnaraghi, F., Wang, G., 2015. Factors influencing the oblique impact test of motorcycle helmets. Traffic Inj. Prev. 16 (4), 404–408.
Finan, J.D., Nightingale, R.W., Myers, B.S., 2008. The influence of reduced friction on head injury metrics in helmeted head impacts. Traffic Inj. Prev. 9 (5), 483–488.
Gadd, C., 1966. Use of a Weighted-Impulse Criterion for Estimating Injury Hazard. SAE Technical Paper 660793.
Golnaraghi, F., Wang, G., Ebrahimi, I. & Jelveh, C., 2012. Impact diverting mechanism. USA, Patent No. US20140189945 A1.
Gennarelli, T.A., Thibault, L.E., Tomei, G., Wiser, R., Graham, D., Adams, J., 1987. Directional dependence of axonal brain injury due to centroidal and non-centroidal acceleration. SAE Tech Paper 872197.
Gurdjian, E., Roberts, V., Thomas, L., 1966. Tolerance curves of acceleration and intracranial pressure and protective index in experimental head injury. J. Trauma 6, 600–604.
Halldin, P., 2011. Helmet. USA, Patent No. US20130042397 A1.
Hardy, W., Mason, M.J., Foster, C.D., Shah, C.S., Kopacz, J.M., Yang, K.H., King, A.I., Bishop, J., Bey, M., Anderst, W., Tashman, S., 2007. A study of the response of the human cadaver head to impact. Stapp Car Crash J. 51, 17–80.
Hibbeler, R.C., 2016. Engineering Mechanics - Dynamics. Pearson Prentice Hall, New Jersey.
Hitosugi, M., Murayama, H., Morozawa, Y., Ishi, K., Ogino, M., Koyama, K., 2014. Biomechanical analysis of acute subdural hematoma resulting from judo. Biomed. Res. (Tokyo) 35 (5), 339–344.
Holbourn, A., Edin, M., Oxfd, D.P., 1943. Mechanics of head injuries. Lancet 242, 438–441.
Ji, S., Zhao, W., Li, Z., McAllister, T., 2014. Head impact accelerations for brain strain-related responses in contact sports: a model-based investigation. Biomech. Model. Mechanobiol. 13, 1121–1136.
Kim, J., Johnston, J.M., Ning, H., Kim, Y., Soni, B., Reynolds, R., Cooper, L., Andrews, J. B., Vaidya, U., 2015. Simulation, fabrication, and impact testing of a novel football helmet padding system that decreases rotational acceleration. Sports Eng. 1 (18), 11–20.
Kimpara, H., Iwamoto, M., 2012. Mild traumatic brain injury predictors based on angular accelerations during impacts. Ann. Biomed. Eng. 40 (1), 114–126.
Kleiven, S., 2007. Predictors for traumatic brain injuries eveluated through accident reconstructions. Stapp Car Crash J. 51, 81–114.
Kleiven, S., 2013. Why most traumatic brain injuries are not caused by linear acceleration but skull fractures are. Front. Bioeng. Biotechnol. 1, 1–5.
Langlois, J., Rutland-Brown, W., Wald, M., 2006. The epidemiology and impact of traumatic brain injury: a brief overview. J. Head Trauma Rehabil. 21 (5), 375–378.
Margulies, S.S., Thibault, L.E., 1992. A proposed tolerrance criterion for diffuse axonal injury in man. J. Biomech. 25 (8), 917–923.
McElhaney, J.H., Roberts, V.L., Hilyard, J.F., Kenkyūjo, N.J., 1976. Properties of human tissues and components: nervous tissues. In: Handbook of human tolerance. Tokyo: Japan Automobile Research Institute Inc., p. 143.
McHenry, B.G., 2004. Head injury criterion and the ATB. Presented at the 2004 ATB Users' Conference. Salt Lake City, UT.
McKee, A.C., Cantu, R.C., Nowinski, C.J., Hedley-Whyte, E.T., Gavett, B.E., Budson, A. E., Santini, V.E., Lee, H.S., Kubilus, C.A., Stern, R.A., 2009. Chronic traumatic enchephalopathy in athletes: progressive tauopathy after repetitive head injury. J. Neuropathol. Exp. Neurol. 68 (7), 709–735.

NOCSAE, 2017. Standard Test Method and Equipment Used in Evaluating The performmance Characteristics of Headgear/Equipment, NOCSAE DOC (ND) 001-17m17b.
NOCSAE, 2017. Standard Performance Specification for Newly Manufactured Football Helmets, NOCSAE DOC (ND) 002-17m17a.
Ommaya, A., Corrao, R., Letcher, F., 1973. Head injury in chimpanzee part 1: biodynamics of traumatic unconsciousness. J. Neurosurg. 39 (2), 152–166.
Ommaya, A., Hirsch, A., 1971. Tolerances for cerebral concussion from head impact and whiplash in primates. J. Biomech. 4 (1), 13–21.
O'Riodain, K., Thomas, P., Phillips, J., Gilchrist, M., 2003. Reconstruction of real world head injury accidents resulting from falls using multibody dynamics. Clin. Biomech. 18 (7), 590–600.
Otte, D., 1991. Technical demands on safety in the design of crash helmets for biomechanical analysis of real accident situations. SAE Tech Paper 912911.
Padgaonkar, A.J., Krieger, K.W., King, A.I., 1975. Measurement of angular acceleration of a rigid body using linear accelerometers. J. Appl. Mech. 42 (3), 552–556.
Pellman, E.J., Viano, D.C., Withnall, C., Shewchenko, N., Bir, C.A., Halstead, P.D., 2016. Concussion in professional football: helmet testing to assess impact performance - part 11. Neurosurgery 58 (1), 78–95.
Phillips, K. D., 1997. Protective Headgear and Protective Armour and a Method of Modifying Protective Headgear and Protective Armour. EU, Patent No. EP0790787 B1.
Pellman, E.J., Viano, D.C., Tucker, A.M., Casson, I.R., 2003. Concussion in professional football: location and direction of helmet impacts - part 2. Neurosurgery 53 (6), 1328–1341.
Pellman, E.J., Viano, D.C., Tucker, A.M., Casson, I.R., Waeckerle, J.F., 2003. Concussion in professional football: reconstruction of game impacts and injuries - part 1. Neurosurgery 53 (4), 799–814.
Prasad, P., Mertz, H., 1985. The position of the United States delegation to the ISO working group 6 on the use of HIC in the automotive environment. SAE Government Industry Meeting and Exposition. Washington, DC.
Rowson, S., Duma, S.M., Beckwith, J.G., Chu, J.J., Greenwald, R.M., Crisco, J.J., Brolinson, P.G., Duhaime, A., McAllister, T.W., Maerlender, A.C., 2012. Rotational head kinematics in football impacts: an injury risk function for concussion. Ann. Biomed. Eng. 40 (1), 1–13.
Rowson, S., Duma, S.M., 2013. Brain injury prediction: assessing the combined probability of concussion using linear and rotational head acceleration. Ann. Biomed. Eng. 41 (5), 873–882.
Siegkas, P., Sharp, D.J., Ghajari, M., 2019. The traumatic brain injury mitigation effects of a new viscoelastic add-on liner. Sci. Rep. https://doi.org/10.1038/s41598-019-39953-1.
Stern, R.A., Riley, D.O., Daneshvar, D.H., Nowinski, C.J., Cantu, R.C., McKee, A.C., 2011. Long-term consequences of repetitive brain trauma: chronic traumatic encephalopathy. Am. Acad. Phys. Med. Rehabil. 3 (10 Suppl 2), S460–S467.
Takhounts, E., Craig, M., Moorhouse, K., McFadden, J., 2013. Development of brain injury criteria (Br IC). Stapp Car Crash J. 57, 243–266.
Zhang, L., Yang, K.H., King, A.I., 2004. A proposed injury threshold for mild traumatic brain injury. J. Biomed. Eng. 126, 226–236.